



**HAL**  
open science

## Minimalistic in-flight odometry based on two optic flow sensors along a bouncing trajectory

Lucia Bergantin, Charles Coquet, Amaury Nègre, Thibaut Raharijaona,  
Nicolas Marchand, Franck Ruffier

► **To cite this version:**

Lucia Bergantin, Charles Coquet, Amaury Nègre, Thibaut Raharijaona, Nicolas Marchand, et al.. Minimalistic in-flight odometry based on two optic flow sensors along a bouncing trajectory. ICCAS 2022 - 22nd IEEE International Conference on Control, Automation and Systems (ICCAS), Nov 2022, Busan, South Korea. 10.23919/ICCAS55662.2022.10003956 . hal-03791733

**HAL Id: hal-03791733**

**<https://hal.science/hal-03791733>**

Submitted on 29 Sep 2022

**HAL** is a multi-disciplinary open access archive for the deposit and dissemination of scientific research documents, whether they are published or not. The documents may come from teaching and research institutions in France or abroad, or from public or private research centers.

L'archive ouverte pluridisciplinaire **HAL**, est destinée au dépôt et à la diffusion de documents scientifiques de niveau recherche, publiés ou non, émanant des établissements d'enseignement et de recherche français ou étrangers, des laboratoires publics ou privés.

# Minimalistic in-flight odometry based on two optic flow sensors along a bouncing trajectory

Lucia Bergantin<sup>1,\*</sup>, Charles Coquet<sup>1</sup>, Amaury Negre<sup>2</sup>, Thibaut Raharijaona<sup>3</sup>, Nicolas Marchand<sup>2</sup> and Franck Ruffier<sup>1</sup>

<sup>1</sup> Aix-Marseille Université, CNRS, ISM, Marseille, 13009 Marseille, France

<sup>2</sup> Gipsa-Lab, CNRS, Université Grenoble Alpes, 38402 Saint-Martin-d’Hères, France

<sup>3</sup> Université de Lorraine, Arts et Métiers Institute of Technology, LCFC, HESAM Université, F-57070 Metz, France

\* Corresponding author: lucia.bergantin@univ-amu.fr

**Abstract**—Estimating the distance traveled while navigating in a GPS-deprived environment is key for aerial robotic applications. For drones, this issue is often coupled with weight and computational power constraints, from which stems the importance of minimalistic equipment. In this study, we present a visual odometry strategy based solely on two optic flow magnitudes perceived by two optic flow sensors oriented at  $\pm 30^\circ$  on either side of a drone’s vertical axis. As results, (i) we measured the local optic flow divergence and the local translational optic flow respectively as the subtraction and the sum of the two optic flow magnitudes perceived (ii) we validated experimentally the visual odometer on a hexarotor oscillating up-and-down while following a 50m-long circular trajectory under three illuminance conditions (117lux, 814lux and 1518lux). The measured optic flow divergence was used to estimate the flight height by means of an Extended Kalman Filter. The estimated flight height scaled the measured translational optic flow, which was integrated to perform minimalistic visual odometry.

## I. INTRODUCTION

The estimation of the 2D position of a drone navigating in an unknown environment in the absence of GPS is a challenging task. One solution is concomitant onboard visual odometry and mapping as well as onboard SLAM (Simultaneous Localisation and Mapping), which requires complex computationally-intensive algorithms [6, 11, 13]. A minimalistic alternative is IMU (Inertial Measurement Unit) based dead reckoning – i.e. an inertial integration – [18]. Navigation strategies based on dead reckoning can be implemented on aerial robots flying from landmark to landmark with prior knowledge of the distances in-between. The dead reckoning position signal can be used by an aerial robot to get close enough to detect a landmark before reaching it, giving a new known starting point. We applied and tested on a hexarotor a method to estimate the distance traveled called SOFIa (Self-scaled Optic Flow time-based Integration model), that has been previously assessed in bio-plausible simulations [2]. The SOFIa method is based on the integration of the translation Optic Flow (OF) scaled by the distance with respect to a surface: the SOFIa method can therefore be seen as an OF-based dead reckoning, without any feedback from the environment (such as detection of a beacon or feedback from a map).

In the case of indoor drones, reducing Size, Weight, and Power (SWaP) of the perception equipment is particularly interesting to estimate the local height and therefore to scale the OF. Thus, the ability to rely only on minimalistic equipment is key. Several strategies based on the use of cameras have been presented, such as performing obstacle avoidance using stereo vision [3, 15, 14] or detecting depth by means of monocular vision [17]. These methods rely on computer vision algorithms, which often require high computational power. A less demanding alternative is the use of OF cues. Several visual odometric approaches involving the use

of OF have been successfully tested on flying robots [9, 19, 5]. All these approaches require ground height information providing the factor scaling the visual information, which is often determined separately by using a static pressure sensor [9] or stereovision [19, 5], for example.

Self-oscillations have been observed in honeybees flying both in horizontal and vertical tunnels ([10] and [16] respectively). The self-oscillatory movement generates a series of expansions and contractions in the OF vector field, known as OF divergence. Previous authors have shown that the changes in vertical speed and flight height make the state vector of an oscillating drone observable [8]. Instabilities due to depth variation have been used to determine the OF scale factor of the observed scene associated with bathymetric information onboard an underwater vehicle [4]. In [1], the local OF divergence was measured by means of two OF magnitudes perceived by two OF sensors set on a chariot performing back-and-forth oscillatory movements in front of a moving panorama. The local OF divergence was then used to estimate the distance between the chariot and the moving panorama by means of an Extended Kalman Filter (EKF).

In this study, we tested the SOFIa method on a hexarotor equipped with two OF sensors oriented downwards flying oscillating up-and-down while following a circular trajectory. Tests were performed in a flying arena under different illuminance conditions and with different oscillation frequencies. We showed that the local OF divergence and the local translational OF can be measured reliably on the hexarotor respectively as the subtraction and as the sum of two OF magnitudes perceived by two OF sensors. The measured local OF divergence was then used to estimate the drone’s flight height by means of an EKF. The estimated flight height scaled the measured local translational OF, which was integrated to perform visual odometry.

In section II, we discuss the method presented to measure the local OF cues. In section III, we discuss the model of the visual odometer. In section IV, we describe the details of the experiments performed. In section V, we show experimentally that it is possible to measure the local OF cues solely on the basis of two OF magnitudes perceived by two OF sensors on the hexarotor. Finally, we used the local OF cues to perform minimalistic in-flight visual odometry.

## II. COMPUTATION OF THE LOCAL OPTIC FLOW CUES BY MEANS OF TWO OPTIC FLOW MAGNITUDES

The translational OF is the pattern generated on the OF vector field by the translational motion of a drone flying above the ground [7]. The local translational OF  $\omega_T^{th}$  can be expressed as the ratio

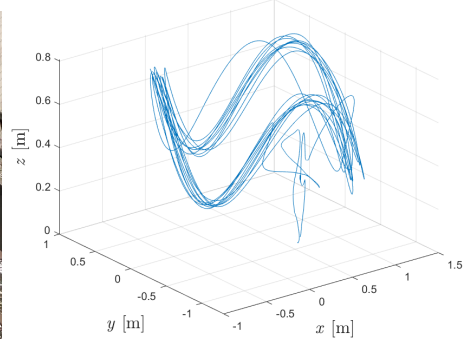
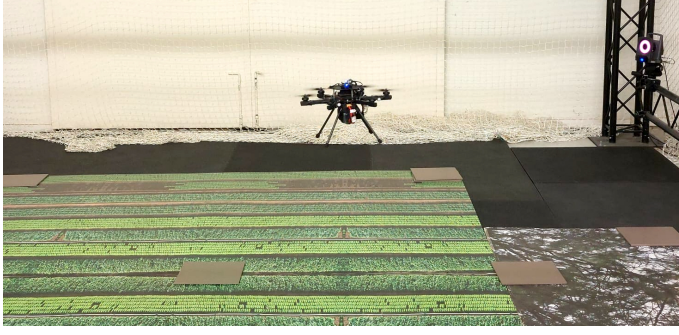


Fig. 1: a) The hexarotor equipped with two Optic Flow (OF) sensors flying along a bouncing circular trajectory in the Marseille’s flying arena. b) Example of the hexarotor’s flight over 53m (3 oscillations per turn at 0.28Hz for a total of 10 turns).

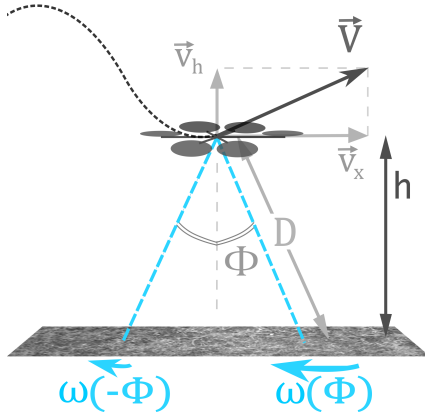


Fig. 2: A hexarotor flies forward while oscillating up-and-down above the ground at a flight height  $h$ . The drone’s velocity  $V$  can be decomposed in the components  $v_x$  and  $v_h$ . The drone is equipped with two Optic Flow (OF) sensors set at angles  $\phi$  and  $-\phi$  with respect to its vertical axis and located at a distance  $D$  with respect to the ground. The OF sensors perceive the OF magnitudes  $\omega(\phi)$  and  $\omega(-\phi)$  respectively.

between the  $v_x$  component of the drone’s velocity and the flight height  $h$  (see Figure 2):

$$\omega_T^{th} = \frac{v_x}{h} \quad (1)$$

We can mathematically demonstrate that the local translational OF can be measured as the sum of two OF magnitudes  $\omega(\phi)$  and  $\omega(-\phi)$  perceived by two OF sensors oriented at angles  $\pm\phi$  with respect to the normal to a surface, divided by a known factor of  $2 \cdot \cos(\phi)^2$  (see mathematical proof in Appendix A):

$$\omega_T^{meas} = \frac{\omega(\phi) + \omega(-\phi)}{2 \cdot \cos(\phi)^2} = \frac{v_x}{h} \quad (2)$$

The series of contractions and expansions generated in the OF vector field by an oscillatory movement is known as OF divergence. When a drone flies forward while oscillating up-and-down above the ground, in the OF vector field the OF divergence is superimposed on the translational OF. Due to the oscillatory movement, the state vector  $X = [h, v_h]^T$  of the drone is locally observable [8] (see Figure 2). The local OF divergence  $\omega_{div}^{th}$  can be expressed as the

ratio between the  $v_h$  component of the drone’s velocity and  $h$ :

$$\omega_{div}^{th} = \frac{v_h}{h} \quad (3)$$

In [1], the authors have mathematically demonstrated that the local OF divergence can be measured as the subtraction between two OF magnitudes  $\omega(\phi)$  and  $\omega(-\phi)$  perceived by two OF sensors oriented at angles  $\pm\phi$  with respect to the normal to a surface, divided by a known factor of  $\sin(2\phi)$ :

$$\omega_{div}^{meas} = \frac{\omega(\phi) - \omega(-\phi)}{\sin(2\phi)} = \frac{v_h}{h} \quad (4)$$

To discard peaks due to noise,  $\omega_{div}^{meas}$  was bounded at  $\pm 2rad/s$ : when  $\omega_{div}^{meas} > 2rad/s$  we considered  $\omega_{div} = 2rad/s$ , while when  $\omega_{div}^{meas} < -2rad/s$  we considered  $\omega_{div} = -2rad/s$ .

### III. THE VISUAL ODOMETER METHOD

In [2], the authors have assessed in simulation a bio-inspired visual odometer called SOFIa (Self-scaled Optic Flow time-based Integration model). The SOFIa model is based on the integration of the local translational OF scaled by the estimates of the distance with respect to the ground  $\hat{h}$ :

$$\hat{X}_{SOFIa} = \int \omega_T \cdot \hat{h} dt \quad (5)$$

In this study, we use the same principle: the translational OF measured as the sum of the two OF magnitudes perceived by the two OF sensors (as in equation (2)) is scaled by the estimates of the flight height  $\hat{h}$  and integrated in order to measure the traveled distance  $\hat{X}_{SOFIa}$  onboard a multirotor.

### IV. MATERIALS AND METHODS

#### A. The hexarotor

We used a hexarotor developed together with Hexadrone<sup>TM</sup>, with as onboard low-level flight controller the PX4 autopilot system [12]. We also used a trajectory tracking algorithm<sup>1</sup> to apply the up-and-down oscillating trajectories on the hexarotor. PX4 is particularly convenient thanks to its adaptability to the nature of the drone (air-wing, quadrotor, hexarotor, etc.) and its reliability when the drone is associated with QGroundControl, a Ground Control Station (GCS), and the MAVLINK protocol. The position and orientation of the drone used in the drone controllers came from the MOCAP system installed in the Marseille’s flying arena. The flying arena was equipped with 17 motion-capture cameras covering a  $6 \times 8$

<sup>1</sup>[https://github.com/gipsa-lab-uav/trajectory\\_control](https://github.com/gipsa-lab-uav/trajectory_control)

$\times 6$  m volume using a VICON<sup>TM</sup> system. Based on the intrinsic attitude stability of the hexarotor, we can consider that there is no rotational component measured by our OF sensors. Furthermore, we consider that pitch and roll are negligible despite the circular bouncing trajectory.

We designed two printed circuit boards to embed the Pixart PAW3903 OF sensors (see Table I), that were set below the hexarotor at  $\phi = \pm 30^\circ$  with respect to its vertical axis as illustrated in Figure 2. The angle  $\phi$  was set at  $30^\circ$  to take into consideration the OF sensors' view-field and the average flight height with respect to the ground. Since we used the VICON MOCAP system as a localisation system, we reported the height of the OF sensors as the drone's flight height.

Each test consisted of a circular trajectory of about 50m with up-and-down oscillations above the ground with an average flight height of 0.55m (see Figure 1). The oscillation peak-to-peak amplitude was 0.5m. Datasets were saved on rosbag files after each test and processed with the Matlab/Simulink 2021 software.

Specifics	OF sensors
OF sensor chip	Pixart PAW3903
OF sensor PCB	$2 \times 2g$
Hardware read-out of the 4 sensors	Arduino Nano

TABLE I: Table of the specifics of the Optic Flow (OF) sensors equipped on the hexarotor.

### B. The Extended Kalman Filter calculations for the estimation of the drone's flight height

We chose to model the hexarotor's system as simply as possible by using a double integrator and by giving the acceleration  $a_z$  on the  $z$  axis available on the drone's IMU as input to the state space model. The hexarotor' state space representation can be expressed as:

$$\begin{cases} \dot{X} = A \cdot X + B \cdot a_z = \begin{bmatrix} 0 & 1 \\ 0 & 0 \end{bmatrix} \cdot X + \begin{bmatrix} 0 \\ 1 \end{bmatrix} \cdot a_z \\ Y = g(X) = [X(2)/X(1)] = v_h/h = \omega_{div} \end{cases} \quad (6)$$

where  $X = [h, v_h]^T$  is the hexarotor's state vector.

To estimate the drone's flight height  $\hat{h}$ , we used an EKF that received as input the acceleration of the drone  $a_z$  and as measurement the local OF divergence  $\omega_{div}^{meas}$  measured as in equation (4). The use of an EKF was necessary due to the non-linearity of the local OF divergence (see equation (3)). See Appendix B for the EKF calculations.

## V. RESULTS

To show experimentally that the signals measured by means of equations (4) and (2) on the hexarotor were indeed respectively the divergence and the translational OF cues, 12 tests were performed at an oscillation frequency of 0.28Hz for each of the following illuminance conditions: 1518lux ( $2.71 \cdot 10^{-4} W/cm^2$ ), 814lux ( $2.15 \cdot 10^{-5} W/cm^2$ ) and 117lux ( $5.36 \cdot 10^{-6} W/cm^2$ ). As shown in Figure 3.a, the values of the measured local OF divergence  $\omega_{div}^{meas}$  of the 12 tests performed at 1518lux pooled together and of the corresponding theoretical local OF divergence  $\omega_{div}^{th}$  (computed as in equation (3)) presented a linear relation, as did those of the measured local translational OF  $\omega_T^{meas}$  and of the corresponding theoretical local translational OF  $\omega_T^{th}$  (computed as in equation (1)). Similar results were obtained for the 12 tests performed at 117lux (see Figure 3.b). Thus, we can use equation (4) to measure

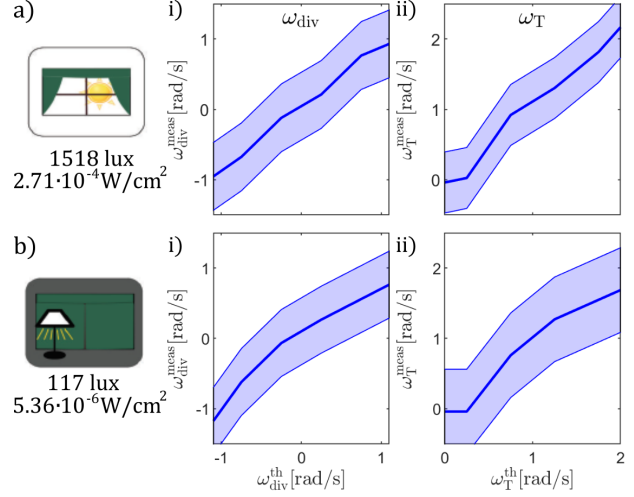


Fig. 3: The plots show the characteristics of the measured Optic Flow (OF) cues with respect to their theoretical counterparts as perceived onboard the hexarotor oscillating vertically at 0.28Hz. The median values and the curves representing the Median Average Deviation (MAD) of the OF cues are shown to display the range of values measured. At 1518lux, the local OF divergence presented a MAD of 0.48rad/s (a.i), while the local translational OF presented a MAD of 0.43rad/s (a.ii). At 117lux, the local OF divergence presented a MAD of 0.47rad/s (b.i), while the local translational OF presented a MAD of 0.6rad/s (b.ii). All plots show linear relations between the measured OF cues and the theoretical OF cues computed under the same illuminance conditions. Therefore, they can be considered as experimental counterparts of the mathematical proofs of equations (4) and (2) respectively.

the local OF divergence cue and equation (2) to measure the local translational OF cue reliably onboard the hexarotor.

The measured local OF divergence  $\omega_{div}^{meas}$  was an oscillating signal slightly distorted as theoretically expected (see example in Figure 4.a). The local OF divergence measured for the 12 tests performed at 1518lux presented a Signal-to-Noise Ratio (SnR, computed as the squared ratio of the root mean square of the signal and the root mean square of its noise) ranging between 4.44dB and 5dB, with a median of 4.86dB. Similar results were obtained for the 12 tests performed at 117lux: the SnR ranged between 4.07dB and 5.14dB, with a median of 4.97dB. As illustrated in Figure 4.a, the estimates of the flight height  $\hat{h}$  obtained by means of an EKF receiving as measurement  $\omega_{div}^{meas}$  converged within 4s to the ground truth  $h$  given by the MOCAP system. Figure 4.b shows the median and the Median Average Deviation (MAD) of the percentage errors of  $\hat{h}$  with respect to  $h$  of all 36 tests pooled together. In particular, for the 12 tests performed at 1518lux the average percentage errors ranged between  $-8.04\%$  and  $3.06\%$ , with a median of  $-2.04\%$  (corresponding to about 0.01m). For the 12 tests performed at 814lux, the average percentage errors ranged between  $-8\%$  and  $6.26\%$ , with a median of  $-2.3\%$  (corresponding to about 0.012m). For the 12 tests performed at 117lux the average percentage errors ranged between  $-2.76\%$  and  $13.52\%$ , with a median of 5.13% (corresponding to about 0.026m).

The measured local translational OF  $\omega_T^{meas}$  was an oscillating signal also slightly distorted as theoretically expected (see example in Figure 5). For the 12 tests performed at 1518lux  $\omega_T^{meas}$  presented

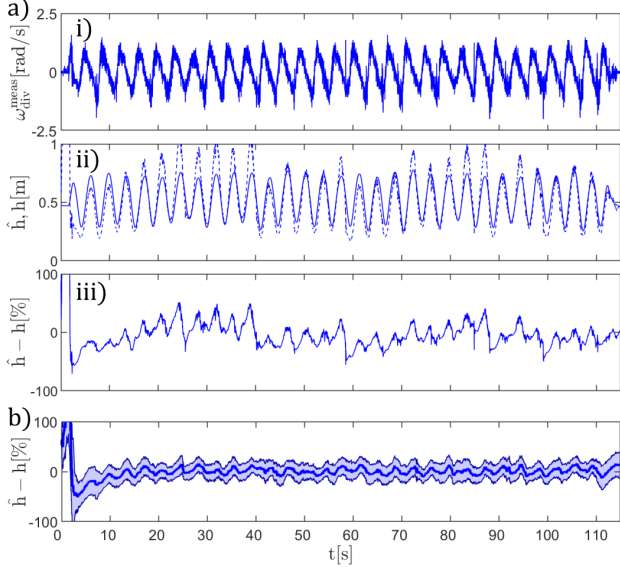


Fig. 4: (a) Example of test performed at 1518lux with an oscillation frequency of 0.28Hz. (i) The measured local Optic Flow (OF) divergence  $\omega_{div}^{meas}$  was an oscillating signal, with a Signal-to-Noise Ratio (SnR) of 4.87dB. (ii)  $\omega_{div}^{meas}$  was used as measurement by the Extended Kalman Filter (EKF) to estimate the hexarotor’s flight height  $\hat{h}$  (in dashed line), which converged within 4s to the ground truth  $h$  (in continuous line). (iii) The percentage error of  $\hat{h}$  with respect to  $h$  ranged between  $-55.39\%$  and  $51.66\%$ , with an average of  $-3.97\%$ . (b) The percentage errors of  $\hat{h}$  with respect to  $h$  of all 36 tests performed at 1518lux, 814lux and 117lux were pooled together: after convergence, they ranged between  $-8.04\%$  and  $13.52\%$ . The median values and the curves representing the Median Average Deviation (MAD) are shown to display the range of percentage errors computed. The MAD after convergence ranged between  $10.04rad/s$  and  $29.57rad/s$ .

a SnR ranging between 23.18dB and 31.15dB, with a median of 26.84dB. Similar results were obtained for the 12 tests performed at 117lux: the SnR ranged between 22.42dB and 27.96dB, with a median of 25.08dB. To assess the accuracy of the visual odometry performed, the final percentage error in the estimates of the distance traveled  $\hat{X}_{SOFIa}$  with respect to the ground truth  $X_{gt}$  traveled along the horizontal component of the circular trajectory was computed. As shown in Figure 6, the final percentage errors of the 12 tests performed at 1518lux had a median of 1.55% (corresponding to about 0.78m), the final percentage errors of the 12 tests performed at 814lux had a median of  $-1.87\%$  (corresponding to about 0.94m), and the final percentage errors of the 12 tests performed at 117lux had a median of 5.04% (corresponding to about 2.52m).

To analyse the robustness of the visual odometry strategy presented to different trajectories, we performed 12 tests at an oscillation frequency of 0.25Hz and 12 tests at an oscillation frequency of 0.31Hz under an illuminance of 1518lux (see Figure 7). At an oscillation frequency of 0.25Hz, the average percentage error of the estimates of  $\hat{h}$  with respect to  $h$  ranged between  $-6.49\%$  and  $10.37\%$ , with a median of  $-2.08\%$ . Similarly, at an oscillation frequency of 0.31Hz the average percentage error ranged between  $-7.14\%$  and  $8.59\%$ , with a median of 4.12%. At 0.25Hz the

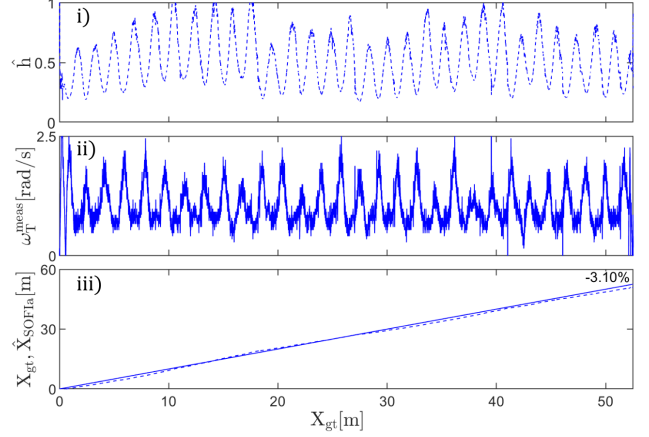


Fig. 5: Example of test performed at 1518lux with an oscillation frequency of 0.28Hz. (i) The estimates of the hexarotor’s flight height  $\hat{h}$  presented an average percentage error after convergence (4s) of  $-3.97\%$ , with a minimum value of  $-55.39\%$  and a maximum value of  $51.66\%$ . (ii) The measured local translational Optic Flow (OF)  $\omega_T^{meas}$  ranged between  $0rad/s$  and  $2.84rad/s$ , with a median of  $0.82rad/s$  and a Signal-to-Noise Ratio (SnR) of 24.98dB. (iii) The estimates of the distance traveled  $\hat{X}_{SOFIa}$  were computed as the integration of  $\omega_T^{meas}$  scaled by  $\hat{h}$  and compared to the ground truth  $X_{gt}$ . The final percentage error of the visual odometry performed was  $-3.10\%$ .

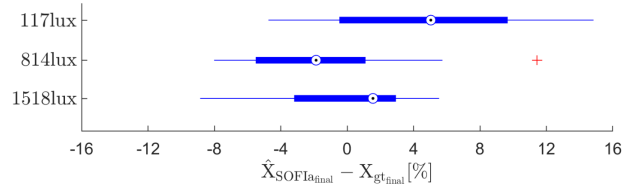


Fig. 6: The error in the estimates of the distance traveled  $\hat{X}_{SOFIa}$  with respect to the ground truth  $X_{gt}$  was expressed in % for all the 36 tests performed with an oscillation frequency of 0.28Hz. For the 12 tests performed at 1518lux the final percentage error ranged between  $-8.85\%$  and  $5.54\%$ , with a median of 1.55%. For the 12 tests performed at 814lux the final percentage error ranged between  $-8\%$  and  $11.44\%$ , with a median of  $-1.87\%$ . For the 12 tests performed at 117lux the final percentage error ranged between  $-4.74\%$  and  $14.83\%$ , with a median of 5.04%.

final percentage error of the odometry had a median of 0.96% (corresponding to about 0.48m), while at 0.31Hz it had a median of 3.37% (corresponding to about 1.69m).

## VI. CONCLUSION

The need to perform visual odometry with minimalistic equipment stems from weight and computational power constraints observed on drones. In this study, we presented a minimalistic visual odometry strategy based solely on the use of two OF sensors placed on a hexarotor at  $\pm\phi$  with respect to its vertical axis. The performance of the minimalistic visual odometry strategy presented was not influenced by illuminance conditions ranging between 117lux and 1518lux. To test the robustness to different trajectories, we performed tests at oscillation frequencies of 0.25Hz, 0.28Hz

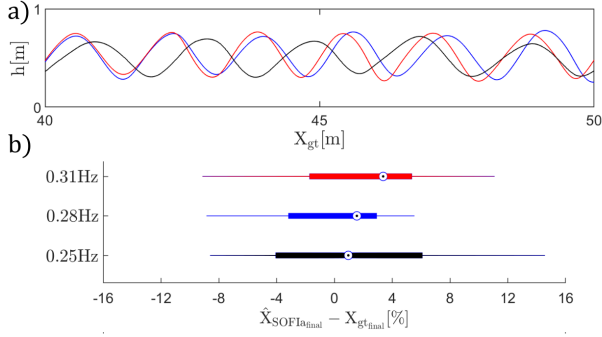


Fig. 7: (a) Examples of test trajectories performed with oscillation frequencies of  $0.25Hz$  (in black),  $0.28Hz$  (in blue) and  $0.31Hz$  (in red) at  $1518lux$ . (b) The error in the estimates of the distance traveled  $\hat{X}_{SOFIa}$  with respect to the ground truth  $X_{gt}$  was expressed in %. For the 12 tests performed at  $0.25Hz$  the final percentage error ranged between  $-8.61\%$  and  $14.58\%$ , with a median of  $0.96\%$ . For the 12 tests performed at  $0.28Hz$  the final percentage error ranged between  $-8.86\%$  and  $5.54\%$ , with a median of  $1.55\%$ . For the 12 test performed at  $0.31Hz$  the final percentage error ranged between  $-9.13\%$  and  $11.09\%$ , with a median of  $3.37\%$ .

and  $0.31Hz$  under an illuminance of  $1518lux$ . The performance of the method presented was similarly accurate for all three oscillation frequencies considered.

The visual odometry strategy presented is interesting for aerial robotic applications in GPS-denied environments, such as buildings or tunnels, to assess the flight distance in order to travel from landmark to landmark. The low weight of the OF sensors and the low computational power required to measure the local OF cues make this method particularly interesting for micro-flyers. We acknowledge that the final traveled distance estimates are subject to a small error as the odometry strategy is a dead-reckoning method without any feedback from the environment. However, such minimalistic OF based odometry strategy would allow a future drone to assess if it comes in proximity of its base station without GPS. For experimental reasons, tests were performed over flat ground. However, previous studies have shown that the SOFIa model is robust to ground irregularities. Thus, future work will include tests in the presence of ground irregularities, such as small slopes, both in the flying arena and outdoors. Future work will possibly include tests under a wider range of illuminance conditions, oscillation frequencies, trajectories and oscillation amplitudes.

#### APPENDIX A

##### COMPUTATION OF THE LOCAL TRANSLATIONAL OPTIC FLOW BY MEANS OF TWO OPTIC FLOW MAGNITUDES

The local translational OF can be measured as the sum of two OF magnitudes  $\omega(\phi)$  and  $\omega(-\phi)$  perceived by two OF sensors oriented at angles  $\pm\phi$  with respect to the normal to a surface, divided by a known factor of  $2 \cdot \cos(\phi)^2$ :

$$\omega_T^{meas} = \frac{\omega(\phi) + \omega(-\phi)}{2 \cdot \cos(\phi)^2} = \frac{v_x}{h} \quad (2)$$

*Proof.* We consider a drone equipped with two OF sensors oriented toward the ground at angles  $\phi$  and  $-\phi$  with respect to its vertical

axis. We can express the OF magnitudes perceived by each OF sensor as:

$$\omega(\phi) = \frac{\|\vec{V}\|}{D} \cdot \sin(\widehat{(\vec{D}, \vec{V})}) = \frac{\|\vec{V}\|}{D} \cdot \sin\left(\frac{\pi}{2} - \phi + \alpha\right)$$

We can express the two components of the velocity vector  $\vec{V}$  of the drone flying above the ground as:

$$\begin{aligned} v_x &= \|\vec{V}\| \cdot \cos \alpha \\ v_h &= \|\vec{V}\| \cdot \sin \alpha \end{aligned}$$

with

$$\|\vec{V}\| = \sqrt{v_x^2 + v_h^2}$$

From which we obtain:

$$\begin{aligned} \cos \alpha &= \frac{v_x}{\sqrt{v_x^2 + v_h^2}} \\ \sin \alpha &= \frac{v_h}{\sqrt{v_x^2 + v_h^2}} \end{aligned}$$

Thus

$$\begin{aligned} \omega(\phi) &= \frac{\|\vec{V}\|}{D} \cdot \sin(\widehat{(\vec{D}, \vec{V})}) \\ &= \frac{\sqrt{v_x^2 + v_h^2}}{D} \cdot \sin\left(\frac{\pi}{2} - \phi + \alpha\right) \\ &= \frac{\sqrt{v_x^2 + v_h^2}}{D} \cdot \left(\sin\left(\frac{\pi}{2} - \phi\right) \cdot \cos \alpha + \cos\left(\frac{\pi}{2} - \phi\right) \cdot \sin \alpha\right) \\ &= \frac{v_x}{D} \cdot \sin\left(\frac{\pi}{2} - \phi\right) + \frac{v_h}{D} \cdot \cos\left(\frac{\pi}{2} - \phi\right) \\ &= \frac{v_x}{D} \cdot \sin\left(\frac{\pi}{2} - \phi\right) + \frac{v_h}{D} \cdot \sin \phi \\ &= \frac{\|v_x\|}{D} \cdot \sin(\widehat{(\vec{D}, v_x)}) + \frac{\|v_h\|}{D} \cdot \sin(\widehat{(\vec{D}, v_h)}) \end{aligned}$$

We can then express the OF magnitudes  $\omega(-\phi)$  and  $\omega(\phi)$  perceived by the two OF sensors as:

$$\omega(-\phi) = \frac{v_x}{D} \cdot \sin\left(\frac{\pi}{2} - \phi\right) - \frac{v_h}{D} \cdot \sin \phi$$

$$\omega(\phi) = \frac{v_x}{D} \cdot \sin\left(\frac{\pi}{2} - \phi\right) + \frac{v_h}{D} \cdot \sin \phi$$

Thus, the local translational OF can be measured as:

$$\omega(\phi) + \omega(-\phi) = 2 \cdot \frac{v_x}{D} \cdot \sin\left(\frac{\pi}{2} - \phi\right)$$

Since  $h = D \cdot \cos(\phi)$  is the distance of the drone from the ground, we obtain:

$$\omega(\phi) + \omega(-\phi) = 2 \cdot \frac{v_x}{h} \cdot \sin\left(\frac{\pi}{2} - \phi\right) \cdot \cos(\phi) \quad (7)$$

By means of the trigonometric formula  $\sin(\frac{\pi}{2} - \phi) = \cos(\phi)$ , we can express equation (7) as follows:

$$\omega_T^{meas} = \omega(\phi) + \omega(-\phi) = \frac{v_x}{h} \cdot 2 \cdot \cos(\phi)^2$$

where  $\omega$  is the OF magnitude,  $\phi$  is the visual direction of the OF sensor with respect to the axis  $z$  and  $h$  is the drone's flight height.  $\square$

APPENDIX B  
EXTENDED KALMAN FILTER CALCULATIONS

The discretized model of the hexarotor (equation (6)) can be expressed as:

$$\begin{cases} X[k+1] = \Phi \cdot X[k] + \Gamma \cdot U[k] \\ Y[k] = C_k \cdot X[k] + D_k \cdot U[k] \end{cases} \quad (8)$$

with

$$\begin{cases} \Phi = e^{A \cdot dt} \\ \Gamma = \left( \int_0^{dt} e^{A \cdot \tau} d\tau \right) \cdot B = (A^T \cdot e^{A \cdot dt} - A^T) \cdot B \\ C_k = h(X_k) = \begin{bmatrix} X_2[k] \\ X_1[k] \end{bmatrix} \\ D_k = 0 \end{cases} \quad (9)$$

where  $dt$  is the discretization time. To estimate the flight height  $h$ , the EKF took the following iterative steps for each  $k^{th}$  time:

**Prediction step**

(a) One-step ahead prediction

$$X_{k/k-1} = \Phi \cdot X_{k-1/k-1} + \Gamma \cdot U_{k-1/k-1} \quad (10)$$

(b) Covariance matrix of the state prediction error vector

$$P_{k/k-1} = \Phi \cdot P_{k-1/k-1} \cdot \Phi^T + Q \quad (11)$$

**Correction step**

(c) Measurement update

$$X_{k/k} = X_{k/k-1} + K_k \cdot (Y_k - H_k \cdot X_{k/k-1}) \quad (12)$$

with  $K_k$  Kalman gain defined as:

$$K_k = P_{k/k-1} \cdot H_k^T \cdot [H_k \cdot P_{k/k-1} \cdot H_k^T + R_k]^{-1} \quad (13)$$

and  $H_k$  Jacobian matrix for the non linear function defined as follows:

$$H_k = \left. \frac{\partial h}{\partial X} \right|_{X=X_{k/k-1}} = \begin{bmatrix} -\frac{\dot{h}}{h^2} & \frac{1}{h} \end{bmatrix} \quad (14)$$

(d) Covariance matrix of state estimation error vector

$$P_{k/k} = P_{k/k-1} + K_k \cdot [H_k \cdot P_{k/k-1} \cdot H_k^T + R_k] \cdot K_k^T \quad (15)$$

(e) Innovation

$$\tilde{Y}_k = Y_k - H_k \cdot X_{k/k} \quad (16)$$

ACKNOWLEDGMENT

We thank J.M. Ingargiola in the design of the printed circuit boards for the OF sensors. Financial support was provided via a ProxyLearn project grant to F.R. from the ANR (Astrid Program). The participation of L.B. in this research project was supported by a joint PhD grant from the Délégation Générale de l'Armement (DGA) and Aix Marseille University. The participation of C.C. was supported by CNRS Innovation via a Prematuration project. L.B, C.C and F.R. were also supported by Aix Marseille University and the CNRS (Life Science, Information Science and Engineering Science & Technology Institutes).

REFERENCES

[1] L. Bergantin, T. Raharijaona, and F. Ruffier. "Estimation of the distance from a surface based on local optic flow divergence". In: *2021 International Conference on Unmanned Aircraft Systems (ICUAS)*. IEEE, 2021, pp. 1291–1298.

[2] L. Bergantin et al. "Oscillations make a self-scaled model for honeybees' visual odometer reliable regardless of flight trajectory". In: *Journal of the Royal Society Interface* 18.182 (2021), p. 20210567.

[3] M. Bertozzi et al. "Stereo vision-based vehicle detection". In: *Proceedings of the IEEE Intelligent Vehicles Symposium 2000 (Cat. No. 00TH8511)*. IEEE, 2000, pp. 39–44.

[4] V. Creuze. "Monocular odometry for underwater vehicles with online estimation of the scale factor". In: *IFAC 2017 World Congress*. 2017.

[5] A. Denuelle and M. V. Srinivasan. "A sparse snapshot-based navigation strategy for UAS guidance in natural environments". In: *2016 IEEE International Conference on Robotics and Automation (ICRA)*. IEEE, 2016, pp. 3455–3462.

[6] M. Faessler et al. "Autonomous, vision-based flight and live dense 3D mapping with a quadrotor micro aerial vehicle". In: *Journal of Field Robotics* 33.4 (2016), pp. 431–450.

[7] J. J. Gibson. *The perception of the visual world*. Houghton Mifflin, 1950.

[8] H. W. Ho, G. CHE de Croon, and Q. Chu. "Distance and velocity estimation using optical flow from a monocular camera". In: *International Journal of Micro Air Vehicles* 9.3 (2017), pp. 198–208.

[9] F. Kendoul, I. Fantoni, and K. Nonami. "Optic flow-based vision system for autonomous 3D localization and control of small aerial vehicles". In: *Robotics and autonomous systems* 57.6-7 (2009), pp. 591–602.

[10] WH Kirchner and MV Srinivasan. "Freely flying honeybees use image motion to estimate object distance". In: *Naturwissenschaften* 76.6 (1989), pp. 281–282.

[11] S. H. Lee and G. de Croon. "Stability-based scale estimation for monocular SLAM". In: *IEEE Robotics and Automation Letters* 3.2 (2018), pp. 780–787.

[12] L. Meier, D. Honegger, and M. Pollefeys. "PX4: A node-based multithreaded open source robotics framework for deeply embedded platforms". In: *2015 IEEE International Conference on Robotics and Automation (ICRA)*. 2015, pp. 6235–6240.

[13] R. Milijas et al. "A comparison of lidar-based slam systems for control of unmanned aerial vehicles". In: *2021 International Conference on Unmanned Aircraft Systems (ICUAS)*. IEEE, 2021, pp. 1148–1154.

[14] R. JD Moore et al. "A stereo vision system for uav guidance". In: *2009 IEEE/RSJ International Conference on Intelligent Robots and Systems*. IEEE, 2009, pp. 3386–3391.

[15] S. Nedeveschi et al. "High accuracy stereo vision system for far distance obstacle detection". In: *IEEE Intelligent Vehicles Symposium, 2004*. IEEE, 2004, pp. 292–297.

[16] G. Portelli et al. "Honeybees' speed depends on dorsal as well as lateral, ventral and frontal optic flows". In: *PLoS one* 6.5 (2011), e19486.

[17] A. Saxena, J. Schulte, A. Y. Ng, et al. "Depth Estimation Using Monocular and Stereo Cues." In: *IJCAI*. Vol. 7. 2007, pp. 2197–2203.

[18] A. Shurin and I. Klein. "QDR: A Quadrotor Dead Reckoning Framework". In: *IEEE Access* 8 (2020), pp. 204433–204440.

[19] R. Strydom, S. Thurrowgood, and M. V. Srinivasan. "Visual odometry: autonomous uav navigation using optic flow and stereo". In: *Proceedings of Australasian conference on robotics and automation*. 2014.